CHIN. PHYS. LETT. Vol. 38, No. 9 (2021) 092901

Low-Temperature Baking Effect of the Radio-Frequency Nb_3Sn Thin Film Superconducting Cavity

Ziqin Yang(杨自钦)[1*], Shichun Huang(皇世春)[1], Yuan He(何源)[1*], Xiangyang Lu(鲁向阳)[2], Hao Guo(郭浩)[1], Chunlong Li(李春龙)[1], Xiaofei Niu(牛小飞)[1], Pingran Xiong(熊平然)[1], Yukun Song(宋玉堃)[1], Andong Wu(吴安东)[1], Bin Xie(谢斌)[1], Zhiming You(游志明)[1], Qingwei Chu(初青伟)[1], Teng Tan(谭腾)[1], Feng Pan(潘峰)[1], Ming Lu(路明)[1,3], Didi Luo(罗迪迪)[1], Junhui Zhang(张军辉)[1], Shenghu Zhang(张生虎)[1], and Wenlong Zhan(詹文龙)[1]

[1]*Institute of Modern Physics, Chinese Academy of Sciences, Lanzhou 730000, China*
[2]*State Key Laboratory of Nuclear Physics and Technology, Peking University, Beijing 100871, China*
[3]*University of Chinese Academy of Sciences, Beijing 100049, China*

(Received 4 July 2021; accepted 28 July 2021; published online 2 September 2021)

The Nb_3Sn thin film cavity, having the potential to be operated at a higher temperature and higher gradient compared to the cavity made from bulk niobium, is one of the most promising key technologies for the next-generation radio-frequency superconducting accelerators. In our work, several 1.3 GHz single-cell TESLA-shaped Nb_3Sn thin film cavities, coated by the vapor diffusion method, were tested at Peking University and Institute of Modern Physics, Chinese Academy of Sciences. It was observed that the performance of the Nb_3Sn thin film cavities in the tests without the slow cooling down procedure and the effective magnetic field shielding was significantly improved by using a low temperature baking at 100 ℃ for 48 hours. Although the peak electric field of the cavity remained unchanged, the rapid drop of the unloaded Q value (Q_0) with the increasing accelerating field (Q-slope) was effectively eliminated, resulting in an improvement of the Q_0 in the intermediate field region by ∼8 times. Furthermore, under better test conditions with the shielded magnetic field less than 5 mG and the slow cooling down procedure in the temperature range of 25–15 K, the Q_0 was still improved by about 20%. Our study shows that the low temperature baking can be an effective supplement to the effective post-treatment for the Nb_3Sn thin film cavity.

DOI: 10.1088/0256-307X/38/9/092901

Radio-frequency superconducting (SRF) accelerators can be operated in long-pulse mode or continuous wave (CW) mode due to the extremely low surface resistance of the SRF cavities. Many accelerator projects under construction and planned, such as a synchrotron radiation source,[1] high energy experimental project,[2] free electron laser,[3] proton and heavy ion accelerator,[4] have chosen to use SRF technology. The SRF cavities for the acceleration of the charged particle are the key components of the SRF accelerators, which are routinely fabricated by high purity niobium (Nb) with a residual resistivity ratio (RRR) larger than 300. After more than half century of development, the performance of the niobium cavities is now approaching their fundamental limits, in terms of both the maximum field and the surface resistance at typical operating temperatures.[5–7] To further reduce the construction and operation cost of the large-scale SRF accelerators, it is of utmost importance to look into alternative materials offering SRF performances beyond Nb.

Compared to the high-purity Nb used for accelerator applications, Nb_3Sn has a theoretical superconducting transition temperature (T_C) of about 18.3 K (∼9.25 K for Nb), an energy gap Δ of about 340 mV (∼140 mV for Nb), and a superheating magnetic field (H_{sh}) of about 425 mT (∼240 mT for Nb).[8] Therefore, the Nb_3Sn thin film SRF cavity can be operated at 4.2 K or even higher temperature, having a theoretical accelerating field two times higher than the Nb SRF cavity. This will not only have a huge impact on the large-scale facilities such as International Linear Collider (ILC), but also make the SRF technology have bright application prospects in small scientific research platforms such as compact light sources[9] and photo-neutron sources,[10] as well as in industrial applications such as wastewater treatment[11] and medical isotope production.[12] In addition, the maximum secondary electron yield (SEY) of Nb_3Sn is very similar to Nb,[8,13] which means that the multipacting

Supported by the Youth Innovation Promotion Association of Chinese Academy of Sciences (Grant No. 2020410), the Major Research Plan of National Natural Science Foundation of China (Grant No. 91426303), the Strategic Priority Research Program of Chinese Academy of Sciences (Grant No. XDB25000000), and the National Postdoctoral Program for Innovative Talents (Grant No. BX201700257).
*Corresponding authors. Email: yzq@impcas.ac.cn; hey@impcas.ac.cn
© 2021 Chinese Physical Society and IOP Publishing Ltd

and field emission behaviors in Nb_3Sn thin film cavities should be comparable to that normally observed in Nb cavities. Thus, the optimized structures of the Nb cavities can be directly applied to the Nb_3Sn cavities. As a result, Nb_3Sn is the most promising new alternative material to Nb for SRF application.

The RF performance of the SRF cavity at cryogenic temperatures significantly depends on the post-treatment process. Many efforts have been made to establish the post-treatment process of the Nb_3Sn thin film cavities. The oxypolishing treatment was explored firstly by Hillenbrand and Martens from Siemens AG,[14–16] of which the Nb_3Sn thin film was anodized in NH_3 solution and the oxide layer was subsequently dissolved in HF solution. The results show that, when the surface layer of the Nb_3Sn thin film is contaminated, the oxypolishing treatment can significantly improve the unloaded quality factor Q_0, otherwise, the oxypolishing treatment has only minor influence on Q_0. Researchers[17] at University of Wuppertal reported a 50% degradation of the low field Q_0 and the onset field of Q-slope after light oxipolishing. Posen[8] repeated the oxypolishing treatment of the Nb_3Sn thin film cavity at Cornell University to remove the possible excess Sn on the surface. However, the Q_0 at low fields was reduced and the Q_0 degradation with the increasing accelerating field (Q-slope) was even stronger at lower fields. The results reported by Siemens AG, University of Wuppertal and Cornell University all show that defects limit the maximum field of the Nb_3Sn thin film cavities. To remove the performance-limiting defect, Posen carried out a light removal of 30–50 nm for the Nb_3Sn thin film by both HF rinse and centrifugal barrel polishing (CBP).[8] However, some residues appeared on the surface of Nb_3Sn grains after the HF rinse, leading to a stronger increase in the Q-slope. The performance degradation after CBP is even more serious than that after the HF rinse. So far, the only effective post-treatment method for Nb_3Sn thin film cavities is high pressure rinsing (HPR) with de-ionized water to prevent field emission.

Previous experience from the Nb cavities indicates that a single effective post-treatment method can only improve the performance of the cavity to some extent. A combination of many effective post-treatment methods must be employed to maximize the RF performance of the cavity.[18] The aim of the present study is to explore and expand the effective post-treatment method for Nb_3Sn thin film cavities. The observation that the low temperature baking treatment after HPR can improve the RF performance of the Nb_3Sn thin film cavities will be reported in detail.

In our work, many 1.3 GHz single cell TESLA shape Nb_3Sn thin film cavities were coated by the vapor diffusion method. The coating process is described as follows: the Nb substrate cavities are heated up in a deposition system with a tin source, as the saturated tin vapor arrives at the inner surface of the cavity and reacts with Nb, a thin layer of Nb_3Sn material at the inner surface of the cavity will be formed.

Before the coating, the 1.3 GHz single-cell TESLA-shaped Nb substrate cavity labeled as X2X4 underwent standard surface treatment of the Nb cavity, including heavy buffered chemical polishing (BCP) of ~130 μm, degassing at 800 ℃ for 3 hours, light BCP of ~20 μm and HPR. Initially, the X2X4 Nb substrate cavity was coated by a recipe adopted from Siemens AG and Jefferson Lab (JLab)[19] with both the Nb cavity and the tin source kept at 1200 ℃ and labeled as X2X4-1.

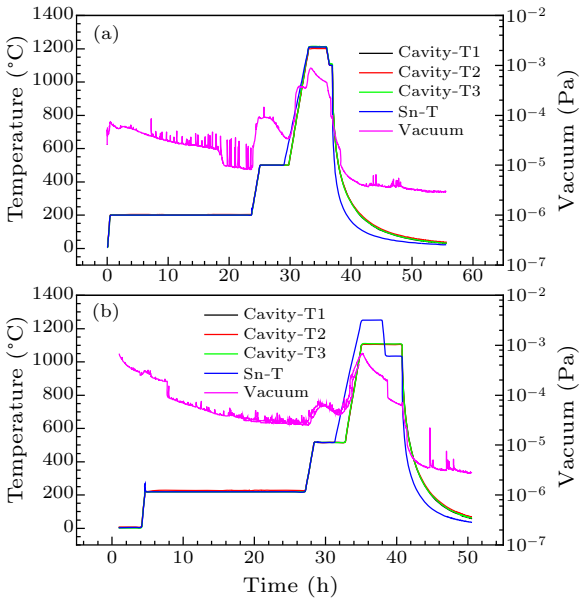

Fig. 1. (a) Recipe of the first coating with both the Nb cavity thermocouples and the tin source thermocouple at 1200 ℃; (b) recipe of the second coating with the Nb cavity thermocouples at 1100 ℃ and the tin source thermocouple at 1250 ℃.

After the vertical tests before and after low temperature baking treatment, the Nb_3Sn thin film of X2X4-1 cavity was removed by BCP with about 40 μm material removal. Then the cavity labeled as X2X4-2 was recoated using a recipe based on the temperatures and times specified by University of Wuppertal[20] and Cornell University,[8] the temperature of the Nb substrate cavity and the tin source recorded by thermocouples were 1100 ℃ and 1250 ℃, respectively. The detailed data of temperature and pressure during the two coating processes are shown in Fig. 1.

Scanning electron microscopy (SEM) experiments were performed on the test samples of both the first coating and the second coating processes to reveal the surface features of the Nb_3Sn thin films. As seen in Fig. 2, the grain size of the Nb_3Sn films grown by the two coatings is 1–2 μm. However, the surface of the

Nb_3Sn film grown during the first coating process has defects such as holes. In contrast, the Nb_3Sn film grown in the second coating process has a smooth surface and full crystal grains. Furthermore, Table 1 shows the EDS spectrum that the average Sn content of the first coating samples is about 22.11 atomic percent, which is obviously smaller than the 23.90% atomic percent tin of the second coating samples.

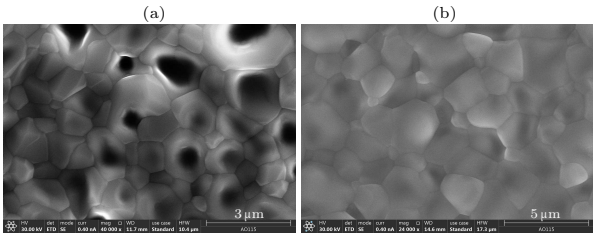

Fig. 2. (a) The surface morphology of the first coating sample (a) and the second coating sample (b).

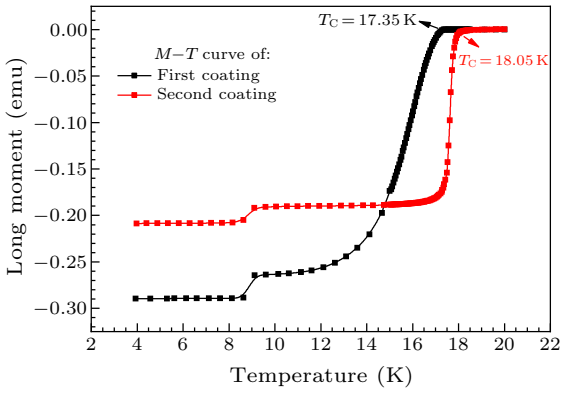

Fig. 3. Magnetization measurements of the Nb_3Sn films.

Table 1. Composition of the Nb_3Sn films coated by the two coating processes.

Coating process	First coating			Second coating		
Position	1	2	3	1	2	3
Sn content (at.%)	22.15	22.03	22.16	23.90	24.02	23.79
Average Sn content	22.11			23.90		

The magnetization was measured using a commercial physical property measurement system (Quantum Design PPMS-9) to determine the superconductivity of the coated Nb_3Sn films, and the results are shown in Fig. 3. For the Nb_3Sn film from the first coating process, the magnetic moments began to decrease rapidly at 17.35 K ($T_{C,onset} = 17.35$ K) and stabilize at 11.59 K ($\Delta T_C = 5.76$ K). $T_{C,onset}$ of the Nb_3Sn film from the second coating process is 18.05 K and its ΔT_C is about 0.76 K. This agrees with the previous studies that a higher Sn content will yield a higher transition temperature.

The difference between the properties of the Nb_3Sn films deposited in the first and the second coating processes is attributed to the difference in the coating conditions. The tin vapor pressure controlled by the temperature of the Sn source determines the rate at which tin arrives at the cavity surface. However, the rate of interdiffusion between niobium and tin is controlled by the cavity temperature. Thus, the recipe of the first coating process led to a lower Sn content, a surface of defects and a smaller film thickness.

The X2X4-1 Nb_3Sn cavity was first tested at Peking University (PKU). Prior to the test, the cavity was treated with HPR to clean the surface. No other treatments were performed. During the test, the magnetic field was effectively shielded below 5 mG, a slow cooldown of about ∼5.2 min/K was achieved from 25 K to 15 K to minimize the thermal current induced magnetic flux, minimizing the contribution of the trapped magnetic flux to the residual resistance of the cavity.[21] The test conditions of PKU are similar to those of Cornell University, JLab and Fermi National Accelerator Laboratory (FNAL). However, the vertical test results in Fig. 5 show that the Q_0 is only $\sim 2.7 \times 10^9$ at 4.2 K in the low field region. Moreover, the Q-slope is serious at the low field region ($E_{acc} < 4$ MV/m), and the maximum accelerating field $E_{acc,max}$ is limited to 7.3 MV/m.

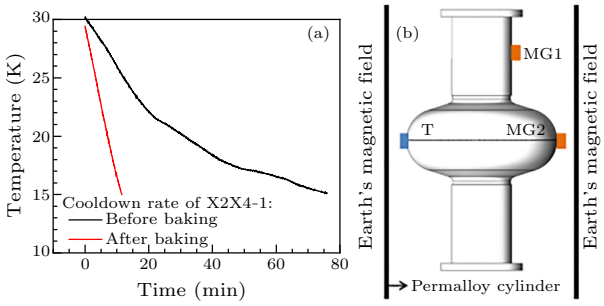

Fig. 4. (a) Cooldown rate of the X2X4-1 Nb_3Sn cavity at IMP before and after low temperature baking treatment. (b) The earth's magnetic field has not been effectively shielded during the test of the X2X4-1 Nb_3Sn cavity at IMP.

After HPR and re-assembly, the X2X4-1 cavity was re-tested at 4.2 K and at IMP. The ambient magnetic field at the equator was as high as 22 mG and the ambient magnetic field near the beam tube even reached 50 mG during the initial test. As depicted in Fig. 4, the cooldown rate crossing 18 K before the low temperature baking is ∼5.5 min/K, which is similar to the rate obtained at PKU. The Q_0 is degraded to $\sim 1.3 \times 10^9$ at a low field region due to the much higher ambient magnetic field. However, the $E_{acc,max}$ up to 10.4 MV/m is achieved as a result of the larger capacity of the cryogenic system at IMP. Nevertheless, the low field Q-slope is still observed.

Based on our previous testing experience, the low field Q-slope may be caused by the insufficient degassing of the cavity. Thus, the cavity was warmed up and *in situ* baked at 100 ℃ for 48 hours at the experimental stand. Then, the cavity was cooled down with a rate of ∼0.8 min/K in the temperature range

of 25–15 K and tested again under the same magnetic shielding conditions as that before baking. Unexpectedly, although the $E_{\mathrm{acc,max}}$ remained unchanged, the Q_0 at low field region was increased to $\sim 4.4 \times 10^9$ as shown in Fig. 5. Furthermore, the low field Q-slope was eliminated and the Q_0 in the intermediate field region was increased by ~8 times.

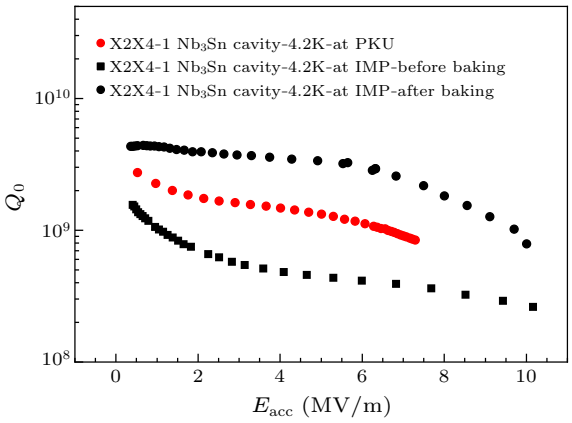

Fig. 5. Significant improvement of the RF performance of the X2X4-1 Nb_3Sn cavity after the low temperature baking at 100 ℃ for 48 hours.

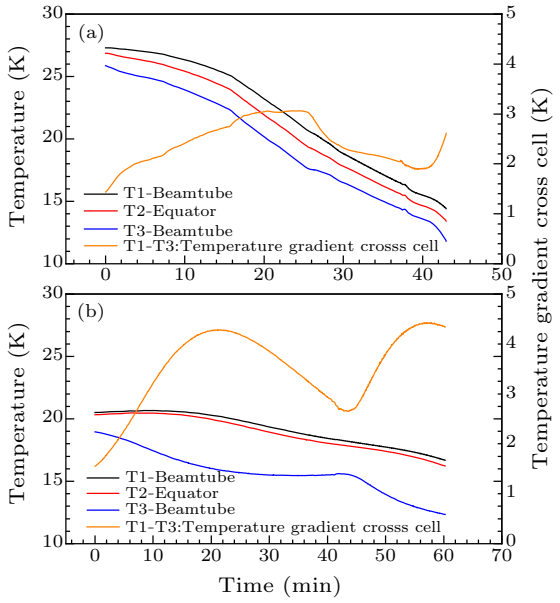

Fig. 6. Vertical test conditions of the X2X4-2 Nb_3Sn cavity before (a) and after (b) low temperature baking treatment.

To further verify the low temperature baking effect of the Nb_3Sn thin film cavity described above, the Nb_3Sn thin film of the X2X4-1 cavity was removed by BCP, recoated and labeled as X2X4-2. After being treated with HPR to clean the surface, the X2X4-2 Nb_3Sn cavity was vertically tested at IMP. It should be noted that the shielded ambient magnetic field is less than 5 mG with the magnetic foil installed inside the testing dewar this time. A cooldown rate of ~2.6 min/K with the temperature gradient of ~2.4 K across the cell was achieved as shown in Fig. 6. On the one hand, the Nb_3Sn film by the second coating has a higher $T_{\mathrm{C,onset}}$ and a smaller ΔT_{C} than that of the first coating process. On the other hand, the vertical test conditions of the X2X4-2 Nb_3Sn cavity is also better than that of the X2X4-1 Nb_3Sn cavity. Therefore, the Q_0 of the X2X4-2 Nb_3Sn thin film cavity at low field reaches 8.8×10^9, degrading to 3.1×10^9 at the quench field of $E_{\mathrm{acc,max}} = 16.11$ MV/m.

Then the X2X4-2 Nb_3Sn cavity was warmed up, removed from the experimental stand to the clean room and baked at 100 ℃ for 48 hours. After the baking, the X2X4-2 Nb_3Sn cavity was vertically tested at 4.2 K again. During this test, the cooldown rate in the temperature range of 25–15 K reached ~11.5 min/K, which is obviously slower than that before baking treatment. However, the X2X4-2 Nb_3Sn cavity was close to the liquid helium injection port, leading to a slightly larger temperature gradient across the cell of 2.7 K. Under such conditions, the Q_0 of the X2X4-2 Nb_3Sn cavity was increased by 11% to 9.8×10^9 at low field, and by about 20% in the field range between 1 MV/m and 8 MV/m. When E_{acc} is greater than 8 MV/m, field emission occurred due to the pollution caused by the exposure of valve sealing interface to the atmosphere during the cavity removal from the experimental stand and its transport to the clean room. Therefore, the X2X4-2 Nb_3Sn cavity after baking exhibited a strong Q-slope above the onset field of $E_{\mathrm{acc}} = 8$ MV/m and quenched at $E_{\mathrm{acc,max}} = 15.51$ MV/m. The comparison of the RF performance of the X2X4-2 Nb_3Sn cavity before and after low temperature baking is shown in Fig. 7.

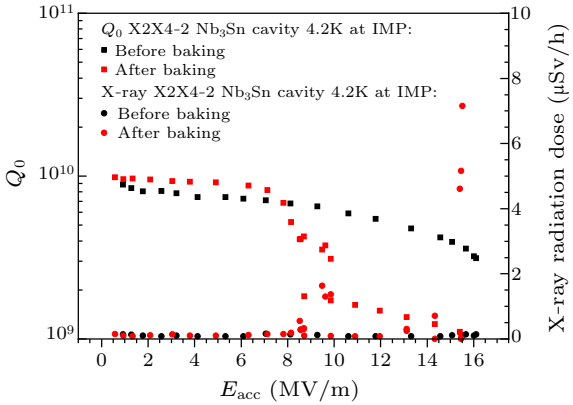

Fig. 7. Vertical test results of the X2X4-2 Nb_3Sn cavity before and after low temperature baking at IMP.

Low temperature baking has become one of the standard post-treatment processes for the pure Nb cavities, and the mechanism has been studied over the past several years, but still remains unclear. Interestingly, we have, for the first time, observed that low temperature baking can improve the RF performance of the Nb_3Sn SRF cavity.

The present research shows that low temperature baking can significantly improve the RF performance of the Nb_3Sn thin film cavities with poor film quality under poor vertical test conditions. In the case of Nb_3Sn thin film cavity with better film quality and under better vertical test conditions, i.e., the magnetic field is shielded below 5 mG, slow cooling can be achieved in the temperature range of 25–15 K, although the performance improvement is small, the performance is still improved after the low-temperature baking.

Research on the mechanism of the low temperature baking effect of the Nb_3Sn thin film cavity is underway. Firstly, the Q_0 of both the X2X4-1 cavity and the X2X4-2 cavity is improved after the low temperature baking, but the maximum accelerating gradient is still the same as before baking, which may be caused by local defects of extremely thin Nb_3Sn layer that cannot fully screen RF currents from Nb implied by both the temperature record and the reference. We can conclude that the low temperature baking may work by changing the surface composition or configuration, not by changing the surface morphology. Secondly, low temperature baking can improve the RF performance of the X2X4-1 cavity more significantly, but the improvement of the X2X4-2 cavity is obviously smaller. As the surface morphology of the test samples shown in Fig. 2, the surface of the test samples from the first coating process has defects such as holes. In contrast, the Nb_3Sn film grown in the second coating process has a smooth surface and full crystal grains. Considering that the inner surface of the Nb_3Sn cavity was treated with HPR prior to the test, dried and then assembled, it is possible that the low temperature baking process may work by removing the water adsorbed on the inner surface of the cavity. The defects such as holes on the inner surface of the X2X4-1 cavity are more likely to absorb water, and it may be difficult to completely remove them by natural drying. This may explain why the low temperature baking has a more significant effect on the X2X4-1 cavity. Thirdly, the RF field is mainly distributed within three penetration depths on the inner surface of the cavity. Therefore, the low temperature baking of Nb_3Sn cavity may also work by affecting surface element composition or material parameters, which has the similar mechanism of the pure Nb cavity.[22]

In summary, this study observes that the low temperature baking can improve the RF performance of the Nb_3Sn cavity, which will be an effective supplement to the effective post-treatments for the Nb_3Sn cavity. The in-depth exploration of the mechanism and comprehensive optimization of the technique of the low temperature baking effect for the Nb_3Sn cavity is being carried out to provide the optimal and reliable low temperature baking conditions. Meanwhile, the low temperature baking may reduce the strict requirements for the coating and operation of the Nb_3Sn cavity, which is of great significance to its engineering application.

For the detailed coating process and material analysis of the test samples, please see the Supplemental Material.

Acknowledgments. The authors are indebted to Jiankui Hao, Lin Lin and Fang Wang at Peking University for their help in the vertical test.

References

[1] Bilderback D H, Elleaume P and Weckert E 2005 *J. Phys. B* **38** S773
[2] Aad G *et al.* 2012 *Phys. Lett. B* **716** 1
[3] Wang D 2018 *Proceedings of ICAP* (America)
[4] He Y, Pan W M, Yue W M *et al.* 2019 *Proceedings of SRF (Germany) MOFAB4*
[5] Grassellino A, Romanenko A, Sergatskov D *et al.* 2013 *Supercond. Sci. Technol.* **26** 102001
[6] Chen S, Hao J K, Lin L *et al.* 2018 *Chin. Phys. Lett.* **35** 037401
[7] Grassellino A, Romanenko A, Trenikhina Y *et al.* 2017 *Supercond. Sci. Technol.* **30** 094004
[8] Posen S 2015 *Understanding and overcoming limitation mechanisms in Nb_3Sn superconducting RF cavities*, PhD Dessertation (Cornell University)
[9] Sei N, Zen H and Ohgaki H 2019 *Phys. Lett. A* **383** 389
[10] Patil B J, Chavan S T, Pethe S N *et al.* 2012 *Appl. Radiat. Isot.* **70** 149
[11] Radiation treatment of gaseous and liquid effluents for contaminant removal, Proceedings of a technical meeting, Sofia, 7-10 September 2004, IAEA, Vienna, 2005, IAEA-TECDOC-1473
[12] Rotsch D A 2016 *Proceedings of NAPAC* (America)
[13] Aull S 2014 *Proceedings of the Sixth International Workshop on Thin Films and New Ideas on RF superconductivity*
[14] Hillenbrand B, Martens H, Pfister H *et al.* 1977 *IEEE Trans. Magn.* **13** 491
[15] Kneisel P, Kupfer H, Schwarz W *et al.* 1977 *IEEE Trans. Magn.* **13** 496
[16] Hillenbrand B 1980 *Proceedings of SRF (Germany) SRF80-3*
[17] Muller G, Kneisel P, Mansen D *et al.* 1996 *Proceedings of EPAC (Spanish) WEP002L*
[18] Yang Z Q 2017 *Study on Nitrogen Doping of High Purity Niobium Used for the Fabrication of Superconducting Radio Frequency Cavity*, PhD Dissertation (Peking University) (in Chinese)
[19] Eremeev G, Reece C E, Kelley M J *et al.* 2015 *Proceedings of SRF (Canada) TUBA05*
[20] Peiniger M, Hein M, Klein N *et al.* 1987 *Proceedings of SRF (America) SRF87E04*
[21] Peiniger M and Piel H A 1985 *IEEE Trans. Magn.* **32** 3610
[22] Trenikhina Y 2015 *Proceedings of SRF* (Canada) WEA1A05

Supplemental Material: Low Temperature Baking Effect of the Nb_3Sn Radio Frequency Superconducting Cavity*

Ziqin Yang(杨自钦)[1**], Shichun Huang(皇世春)[1], Yuan He(何源)[1**], Xiangyang Lu(鲁向阳)[2], Hao Guo(郭浩)[1], Chunlong Li(李春龙)[1], Xiaofei Niu(牛小飞)[1], Pingran Xiong(熊平然)[1], Yukun Song(宋玉堃)[1], Andong Wu(吴安东)[1], Bin Xie(谢斌)[1], Zhiming You(游志明)[1], Qingwei Chu(初青伟)[1], Teng Tan(谭腾)[1], Feng Pan(潘峰)[1], Ming Lu(路明)[1,3], Didi Luo(罗迪迪)[1], Junhui Zhang(张军辉)[1], Shenghu Zhang(张生虎)[1], and Wenlong Zhan(詹文龙)[1]

[1]*Institute of Modern Physics, Chinese Academy of Sciences, Lanzhou 730000*

[2]*State Key Laboratory of Nuclear Physics and Technology, Peking University, Beijing 100871*

[3]*University of Chinese Academy of Sciences, Beijing 100049*

The detailed coating process

The Nb substrate cavity is heated in a deposition system with a tin source, during which the saturated tin vapor arrives at the inner surface of the cavity and reacts with Nb to form a thin layer of Nb_3Sn material. There are two heating zones in our deposition system for Nb cavity and tin source, respectively. This allows for separate temperature control of the Nb substrate cavity and the tin source. The test samples were coated with Nb_3Sn thin film together with the Nb substrate cavity.

Before the coating, the 1.3GHz single-cell TESLA-shaped Nb substrate cavity labeled as X2X4 underwent standard preparation including heavy buffered chemical polishing (BCP) of ~130μm, degassing at 800^0C for 3 hours, light BCP of ~20μm and HPR. Initially, the X2X4 Nb substrate cavity was coated by a recipe adopted from Siemens AG and Jefferson Lab (JLab) and labeled as X2X4-1. The substrate Nb cavity along with the test samples were lowered into the deposition system. After the degassing stage at 200^0C for 24 hours, both the cavity and the tin source were heated to 500^0C to the nucleation stage. During the nucleation stage, the evaporated $SnCl_2$ saturated vapor reached the surface of substrate Nb and formed Sn nucleation sites. After that, both the Nb cavity thermocouples and the tin source thermocouple were heated to 1200^0C for the coating step. After 3 hours, the temperature was dropped to 1100^0C and lasts for 30 minutes to give residual tin on the surface time to diffuse into the surface and react before turning off the furnace, which is called the annealing step. Then the deposition system was powered off, the cavity was carefully removed and vertically tested.

After the vertical test before and after low temperature baking treatment, the thin film of X2X4-1 Nb_3Sn cavity was removed by BCP with the removal amount of 40μm. Then the cavity was recoated using a recipe based on the temperatures and times specified by the University of Wuppertal and Cornell University. The parameters of degassing and nucleation stages are the same as those of the first coating process described above. However, at the coating step, the thermocouples of Nb cavity and tin source was heated to 1100^0C and 1250^0C, respectively. Three hours later, the tin source thermocouple was reduced to 1035^0C and the annealing step lasts for 3 hours. Then the deposition system cooled down naturally and the newly coated Nb_3Sn cavity was prepared for vertical test.

Material analysis of the test samples

The X-ray diffraction (XRD) analysis was performed to detect the surface compositions of the Nb_3Sn thin films. The X-ray powder diffraction patterns of the test samples from the first coating and the second coating process were shown in Fig. S1. Peaks heights have been

normalized with respect to the strongest one and the graphs abscissa range goes from 10 to 90^0. It can be seen that all the peaks have been associated to the Nb_3Sn phase and no undesired low-Tc phases such as $NbSn_2$, Nb_6Sn_5 were detected.

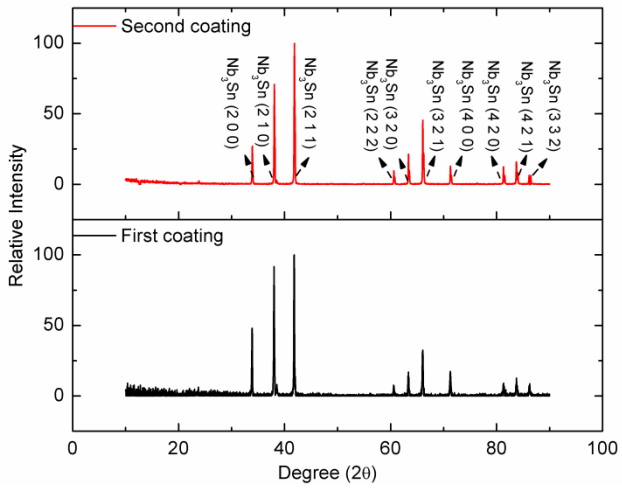

Fig. S1 X-ray powder diffraction patterns of the test samples from the first coating and the second coating.

The thickness of the Nb_3Sn film was measured by using a focused ion beam (FIB), during which steep trenches were etched so that SEM could be used to look at the layers in profile. The FIB-SEM measurements in Fig. S2 showed that the thickness of the Nb_3Sn films from the first and second coating process was ~2.23μm and ~3.01μm, respectively. This is consistent with the depth profiles of Sn^+/Nb^+ ratio by the time of flight secondary ion mass spectrometry (TOF-SIMS) measurements in Fig. S3.

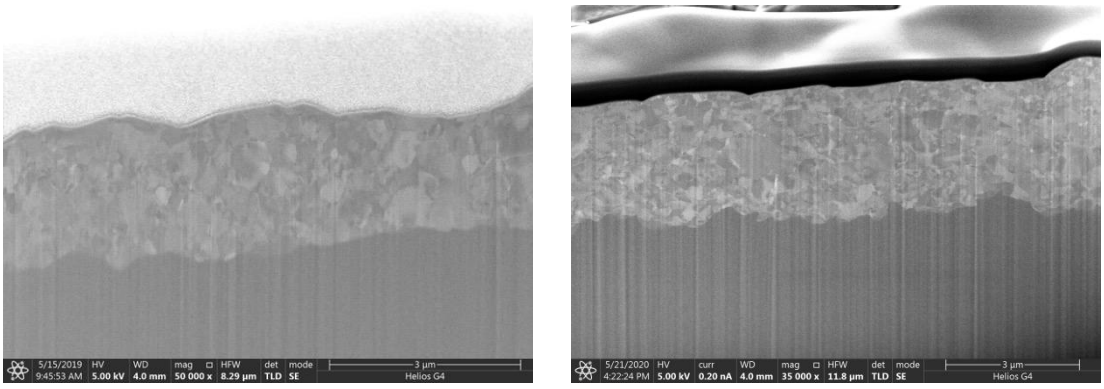

(a) (b)

Fig. S2 FIB-SEM measurement shows that the thickness of the Nb_3Sn films from the first coating (a) is ~2.23μm, and that from the second coating (b) is ~3.01μm.

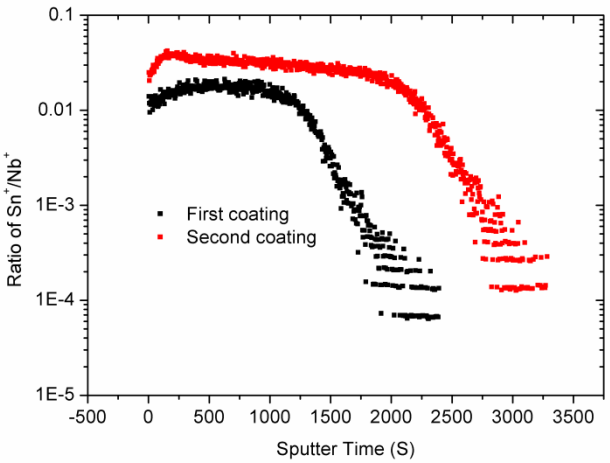

Fig. S3 Depth profiles of the Sn^+/Nb^+ ratio of the test samples.

The difference between the properties of the Nb_3Sn films deposited in the first and second coating process is due to the difference in the coating conditions. The tin vapor pressure is controlled by the temperature of the Sn source and therefore determines the rate at which tin arrives at the cavity surface. However, the rate of interdiffusion of niobium and tin is controlled by the cavity temperature. Thus, the recipe of the first coating resulted in a lower Sn content, a surface of defects and a smaller film thickness.